AGU PUBLICATIONS

Geophysical Research Letters

RESEARCH LETTER
10.1002/2016GL071951

Key Points:
- Using Bayesian techniques for three different lightning data sets provides a better estimate of performance
- The maximum global stroke detection efficiency of Vaisala is 59.8%, ENTLN 56.8%, and WWLLN 7.9%
- Merging the three data sets suggests that there are at least 90.1 strokes or pulses every second

Supporting Information:
- Supporting Information S1

Correspondence to:
P. M. Bitzer,
pm.bitzer@uah.edu

Citation:
Bitzer, P. M., and J. C. Burchfield (2016), Bayesian techniques to analyze and merge lightning locating system data, *Geophys. Res. Lett.*, *43*, 12,605–12,613, doi:10.1002/2016GL071951.

Received 12 JUL 2016
Accepted 29 NOV 2016
Accepted article online 5 DEC 2016
Published online 26 DEC 2016

Bayesian techniques to analyze and merge lightning locating system data

Phillip M. Bitzer[1] and Jeffrey C. Burchfield[2]

[1]Department of Atmospheric Science, University of Alabama in Huntsville, Huntsville, Alabama, USA, [2]Earth Systems Science Center, University of Alabama in Huntsville, Huntsville, Alabama, USA

Abstract As more lightning locating systems (LLSs) become available, there is a growing need to assess how each LLS performs and how to best merge data from multiple LLSs. A Bayesian analysis is used to compare the worldwide data of LLSs from three providers for November 2014 to October 2015: Earth Networks Total Lightning Network (ENTLN, Earth Networks), the combined data from the Global Lightning Detection 360 and National Lightning Detection Network (Vaisala), and the World Wide Lightning Location Network (WWLLN, University of Washington). By using the union of the data sets we are able to determine an estimate for the upper limit of the absolute detection efficiency of each system. Globally, ENTLN detected 56.8% of the discharges, the combined Vaisala networks detected 59.8%, and WWLLN detected 7.9%. In addition, there were 2.842×10^9 unique discharges detected by these LLSs, an average of 90.1 strokes/s.

1. Introduction

Lightning data from various lightning locating systems (LLSs) has been used to assess climatological variations [e.g., *Reeve and Toumi*, 1999; *Boccippio et al.*, 2001; *Christian et al.*, 2003; *Williams*, 2005; *Cecil et al.*, 2012; *Koshak et al.*, 2015], global electrical properties [e.g., *Blakeslee et al.*, 2014; *Mach et al.*, 2011], severe weather dynamics and operational meteorology [e.g., *MacGorman et al.*, 1989; *Carey and Rutledge*, 2003; *Steiger et al.*, 2007; *Schultz et al.*, 2009; *DeMaria et al.*, 2012; *Bruning and MacGorman*, 2013; *Calhoun et al.*, 2013; *Schultz et al.*, 2015], and other applications. In addition, investigations into atmospheric electricity phenomena such as sprites [*Lu et al.*, 2012; *Cummer et al.*, 2013] and terrestrial gamma ray flashes [*Briggs et al.*, 2013; *Connaughton et al.*, 2010] exploit LLSs to further qualify the associated processes. Further, the application of lightning data in operational meteorology is expanding; understanding the characteristics of a LLS will be critical for high impact events [*Goodman et al.*, 2013; *Calhoun et al.*, 2014, and references therein]. Hence, the understanding of how well an LLS performs is vital, and a more robust measure of total lightning (both cloud-to-ground and intracloud) is desired.

Nominally, an estimate of the detection efficiency of a LLS is used to document how well the LLS detects all lightning. This is usually done by some form of ground truth [*Jerauld et al.*, 2005; *Nag et al.*, 2011; *Poelman et al.*, 2012; *Mallick et al.*, 2015] or comparing two LLSs with each other [*Said et al.*, 2010; *Abarca et al.*, 2010; *Pohjola and Mäkelä*, 2013; *Rudlosky and Shea*, 2013; *Thompson et al.*, 2014; *Nag et al.*, 2015; *Bitzer et al.*, 2016]. The latter is usually done by treating one as "truth," and the detection efficiency for one LLS is found. More formally, this type of analysis usually results in the conditional probability that one LLS detects a discharge, given that another LLS detected the same discharge.

Recently, *Bitzer et al.* [2016] formalized an approach in which Bayesian methods are applied to the problem. This extends the usual comparison by considering not only the conditional probability that system A detects a lightning discharge given that system B detected it but also the "reverse" problem: the conditional probability that system B detects a lightning discharge given that system A detected it. This approach is beneficial since it does not assume either LLS detects all lightning. In this manner, an upper estimate for the absolute detection efficiency (DE) for each system can be found.

The Bayesian approach has the added benefit of also identifying how data from LLSs can be merged. For example, this could be exploited to combine LLSs that have spatially varying detection efficiencies or different sensitivities to the type of discharge (e.g., intracloud or cloud to ground) to get a more comprehensive estimate of lightning activity. The Bayesian methodology provides a statistically rigorous approach to the problem. In terms of probability theory, the merged data are given by the union of the two data sets.

This has important implications as more LLSs are developed and become operational. For example, the Geostationary Lightning Mapper (GLM) is scheduled for launch in November 2016. The methodology described herein can be used to combine various ground-based systems to provide a more complete reference data set by which GLM can be validated. In addition, researchers and operational users can use this approach to form a more thorough analysis of lightning activity. This is particularly useful because GLM is expected to perform similarly to the Lightning Imaging Sensor (LIS). Since LIS, and by extension GLM, is generally more sensitive to intracloud lightning [*Thomas et al.*, 2000], while long-range ground based systems are more sensitive to cloud-to-ground lightning [e.g., *Cummins and Murphy*, 2009], a merged data set can provide a better picture of total lightning activity.

This work extends the approach of *Bitzer et al.* [2016] to analyze three different LLSs. First, using Bayesian methodology we merge two Vaisala data sets: the National Lightning Detection Network (NLDN) [*Cummins and Murphy*, 2009] and the Global Lightning Detection 360 network (GLD360) [*Said et al.*, 2013], henceforth referred to as the Vaisala (VAI) data set. Then, the Earth Networks Total Lightning Network (ENTLN) [*Liu and Heckman*, 2012], the merged Vaisala Networks, and the World Wide Lightning Location Network (WWLLN) [*Rodger et al.*, 2005; *Virts et al.*, 2015] are analyzed for a full year: November 2014 to October 2015. Each of the LLSs are sensitive to impulsive, large-scale discharges such as return strokes, K changes [*Kitagawa and Brook*, 1960], and other high current in-cloud discharges; these are the base units of measurement provided by each system. Herein we use the term "strokes/pulses" to refer to the discharges detected by a LLS. In addition, the data provided by each LLS have temporal precision of 1 μs or better. We assume that the percentage of false detections from each LLS is minimal; hence, false detections would only nominally affect the results.

2. Methodology

To compare, and then merge, three different LLSs, we begin with the union of the data from each LLS:

$$P\left(A_1 \cup A_2 \cup A_3\right) = \sum_{i=1}^{3} P\left(A_i\right) - P\left(A_{12}\right) - P\left(A_{23}\right) - P\left(A_{13}\right) + P\left(A_{123}\right), \tag{1}$$

where A_i are the data from the ith LLS, $P\left(A_i\right)$ is the probability that the ith LLS detected the discharge, and we adopt the notation $A_{ij} \equiv A_i \cap A_j$, $A_{ijk} \equiv A_i \cap A_j \cap A_k$, i.e., the intersection of the various data sets.

Using a combination of Bayes' Theorem

$$P(A \mid B) = P(B \mid A)\frac{P(A)}{P(B)} \tag{2}$$

and the multiplicative law,

$$P(A \mid B) = \frac{P(A \cap B)}{P(B)}, \tag{3}$$

equation (1) can be rewritten as

$$P\left(A_1 \cup A_2 \cup A_3\right) = \alpha_1 P\left(A_1\right) \tag{4}$$

where

$$\alpha_1 = 1 + P\left(A_2 \mid A_1\right)\left[\frac{1}{P\left(A_1 \mid A_2\right)} - 1\right] + P\left(A_3 \mid A_1\right)\left[\frac{1}{P\left(A_1 \mid A_3\right)}\left\{1 - P\left(A_2 \mid A_3\right)\right\} - 1\right] + P\left(A_{23} \mid A_1\right) \tag{5}$$

Similar expressions relating the union of the three data sets to A_2 and A_3 via α_2 and α_3 are found through the appropriate application of Bayes' Theorem and the multiplicative law. Hence, the union of the data from three LLSs can be written in terms of the pairwise conditional probabilities. Notably, the conditional probabilities (e.g., $P\left(A_2 \mid A_1\right)$) are similar to the values traditionally derived when comparing LLSs to find the relative detection efficiency.

Table 1. Summary of the Individual Conditional Probabilities

Conditional Probabilities	Values
P(VAI|ENTLN)	0.323
P(WWLLN|ENTLN)	0.094
P(VAI ∩ WWLLN|ENTLN)	0.060
P(ENTLN|VAI)	0.307
P(WWLLN|VAI)	0.072
P(ENTLN ∩ WWLLN|VAI)	0.057
P(ENTLN|WWLLN)	0.671
P(VAI|WWLLN)	0.546
P(ENTLN ∩ VAI|WWLLN)	0.432

In practice, the algorithm to carry out this analysis is straightforward. The conditional probability $P\left(A_2|A_1\right)$ that A_2 detects a discharge, given that A_1 detects a discharge is found. Then, the reverse conditional probability is found, i.e., $P\left(A_1|A_2\right)$ Similarly, $P\left(A_3|A_1\right)$ and $P\left(A_1|A_3\right)$ are determined. When finding the conditional probability that A_2 detects a discharge given that A_3 detected it, the intersection of these data sets, $P\left(A_2|A_3\right)$, is also calculated. In turn, this is used to find the conditional probability that both A_2 and A_3 detected the discharge, given A_1 detected it, $P\left(A_{23}|A_1\right)$. These results are then used to find α_1 in equation (5).

If at least one of the LLSs detects all lightning, the probability of the union is one; in practice, this is usually not the case. Hence, the maximum probability of the union of the three data sets is unity. Thus, the upper limit for the absolute probability (detection efficiency) $P\left(A_1\right)$ is then given by

$$P\left(A_1\right) \leq \frac{1}{\alpha_1}. \tag{6}$$

Using a similar approach to find α_2 and α_3 yields upper limits for $P\left(A_2\right)$ and $P\left(A_3\right)$. Herein we will refer to these as the absolute probabilities (or detection efficiencies) with the understanding that it is the upper limit. Unlike *Rubinstein* [1994] which assumed that the probability of the detection of a discharge was the same, and therefore independent, within each LLS, this work makes no such a priori assumption.

In this analysis, we compare stroke/pulse data from each system. Since this is the basic unit detected by each system, it yields a fundamental assessment of the abilities of the various LLSs. In addition, use of stroke/pulse data allows for tighter temporal and spatial constraints when doing the matching, i.e., determining the conditional probabilities. This ensures quality matching between the various LLSs. However, the extension to flash data would follow the same methodology, albeit with different constraints for the matching.

We tested various spatial and temporal matching constraints used to determine if two data sets detect the same discharge and find the conditional probability. Ultimately, the analysis herein used 50 μs and 25 km. These constraints yielded distributions of the time and distance differences of the matched discharges in which the tails were essentially zero (not shown). Increasing the constraints to 100 μs and 35 km changed the absolute probabilities by less than two percentage points. Other results (e.g., the absolute probabilities) in this manuscript were changed by similar nominal amounts.

Since the two Vaisala LLSs, NLDN, and GLD360, are provided as separate data sets, we first find the union (referred to herein as VAI or Vaisala) following the Bayesian analysis scheme in *Bitzer et al.* [2016]. The GLD360 data have been postprocessed to incorporate an updated (now used operationally) algorithm [*Said and Murphy*, 2016]. In total, GLD360 detected 1.586×10^9 strokes, while NLDN detected 2.50×10^6 strokes (or pulses). Strokes/pulses that are located within 30 μs and 25 km by each system are considered to be the same discharge. The tails of the time and distance distributions of the matches were essentially zero at these constraints. The constraints are smaller than those used in the analysis of the three LLSs because of the errors for these systems in North America; however, when using the same constraints as in the three LLS analysis, the results only differed by a few percentage points. We found, globally, P(NLDN|GLD360) = 0.081 and P(GLD360|NLDN) = 0.513. The average time difference between the matches was 1.8 μs (standard deviation 10.2 μs); the average distance difference was 3.33 km (standard deviation 2.95 km). In total, there were 1.708×10^9 unique discharges detected by the two Vaisala data sets.

3. Results

3.1. Global Statistics

We begin by finding each conditional probability globally. These are summarized in Table 1. The largest of these, P(ENTLN|WWLLN), might be expected since ENTLN uses WWLLN waveforms in some solutions

Table 2. Summary of the Upper Limit of the Absolute Detection Efficiencies

Upper Limit	Value
P(ENTLN)	0.568
P(VAI)	0.598
P(WWLLN)	0.079

[*Rudlosky*, 2015]. Using the conditional probabilities, α_1, α_2, and α_3 are determined, and in turn, the upper limits of the absolute DE for each LLS is calculated. On a global scale, the Vaisala LLS detected 59.8% of the discharges detected by any of the three LLSs (Table 2). The two-system comparisons illustrate the utility in using three LLSs in determining the upper limit of the absolute probability. For example, using just ENTLN and WWLLN to estimate the absolute DE yielded $P(\text{ENTLN}) = 0.956$ and $P(\text{WWLLN}) = 0.134$. In other words, of the discharges detected by ENTLN and WWLLN, ENTLN detected 95.6%. When doing the three-system comparison, ENTLN detected 56.8%. This implies that the addition of the Vaisala data set includes a significant set of discharges not detected by ENTLN or WWLLN; hence, the three-system comparison yields a more accurate measure of the upper limit of the absolute DE. Notably, the two-system comparison between Vaisala and ENTLN yielded $P(\text{VAI}) = 0.608$ and $P(\text{ENTLN}) = 0.578$, similar to the three-system results.

The mean difference in time found when determining the conditional probabilities ranged from 0.2 μs (for ENTLN|WWLLN) to 4.5 μs (for (VAI∩WWLLN)|ENTLN), and the standard deviations ranged from 15 to 19 μs. The mean difference in location ranged from 3.8 km (for ENTLN|WWLLN) to 6.9 km (for VAI|WWLLN), and the standard deviations ranged from 4.1 to 4.7 km. Hence, times and locations of discharges detected by multiple systems are largely similar on a storm scale.

3.2. Spatial Variation

To further explore differences in the LLSs, we analyze the spatial distribution of the absolute DEs. To visualize the DE of each LLS simultaneously, we utilize a RGB map (Figure 1). In this scheme, the value of each component of the colors is proportional to the DE of that LLS. Herein we associate ENTLN with red, Vaisala with

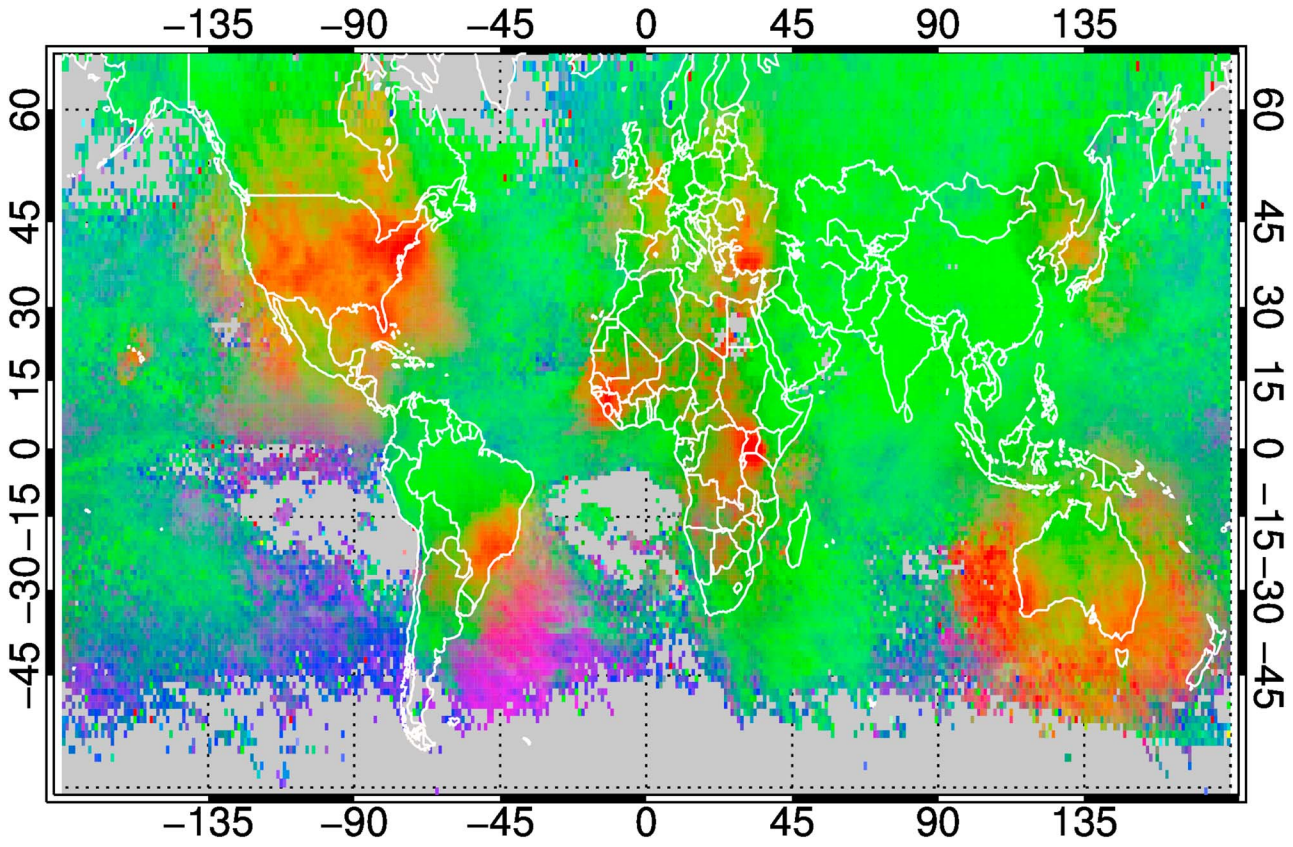

Figure 1. The spatial distribution of the upper limit of the absolute detection efficiency of each LLS. In this RGB map, the value of the red in each 1° × 1° pixel is proportional to the absolute DE of ENTLN, the value of the green in each pixel is proportional to the absolute DE of Vaisala, and the value of the blue in each pixel is proportional to the absolute DE of WWLLN. Pixels in which there are fewer than 50 discharges detected are gray.

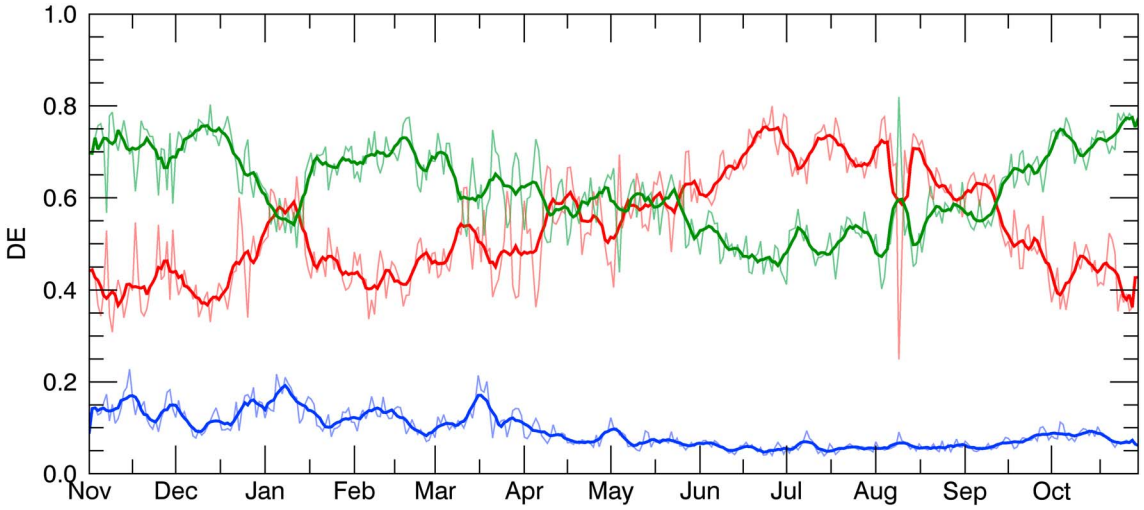

Figure 2. The daily variation of the absolute DE for ENTLN (red), Vaisala (green), and WWLLN (blue). The lighter weight lines are the daily probabilities, while the heavier weight lines are the 7 day moving average of the probabilities.

green, and WWLLN with blue. Regions in the northeastern United States, near Sao Paulo, Brazil, and portions of Africa that have pixels that are predominately red indicate those of the discharges detected by all three systems, ENTLN had the highest DE. Green pixels, such as across Asia, northern Canada, and northern South America, indicate that Vaisala had the highest DE. Off the eastern coast of South America, the purple pixels mean that WWLLN and ENTLN have roughly the same DE (equal proportions of red and blue). The supporting information contains the DE of each LLS as a separate map for reference.

3.3. Temporal Variation

In addition, we found the temporal trend of the absolute probability of each LLS (Figure 2). This is done by calculating the probabilities for each day in the data set. Because of the Bayesian nature of the analysis, these are highly coupled. For completeness, the daily count plot detected by each system can be found in the supporting information.

There is a low-frequency variation in the trends, particularly for ENTLN and Vaisala. Beginning in April, the ENTLN absolute probability increased and the Vaisala DE decreased until August. During this period, the WWLLN DE decreased to below 10%. There can also be significant high-frequency fluctuations in the trends. For example, there was a rapid decrease in the ENTLN probability in August. At this time, the Vaisala and WWLLN probabilities increased. This coincides with a rapid decrease in the number of lightning discharges detected by ENTLN (Figure S4 in the supporting information).

3.4. Merging LLS Data

Besides providing a methodology to assess each LLS without assuming any single LLS is the "truth," the Bayesian analysis can also be used to find the number of unique lightning discharges detected, given by the union of the LLS data sets. This can be obtained via tracking the matches ("hits") and nonmatches ("misses") when finding the conditional probabilities. One such combination that gives the union is

$$A_1 \cup A_2 \cup A_3 = h_{1|2} + h_{23|1} - h_{2|3} + m_{1|2} + m_{2|1} + m_{1|3} \tag{7}$$

where $h_{i|j}$ is the number of hits when finding $P\left(A_i|A_j\right)$ and $m_{i|j}$ is the number of misses.

For the time period of this analysis, ENTLN detected 1.621×10^9 discharges, Vaisala detected 1.708×10^9, and WWLLN detected 0.226×10^9. The total number of unique lightning discharges detected by the three LLSs is 2.842×10^9, which differs from the arithmetic sum by 25%. Thus, the stroke/pulse rate globally determined from these LLSs was 90.1 strokes/s.

Besides the difference in the overall counts, the unioned data provide a better estimate of the total lightning produced by combining LLSs that have performances that may vary in space and/or time. Figure 3 shows the spatial distribution of the unique lightning detected for this time period. When combined with Figure 1

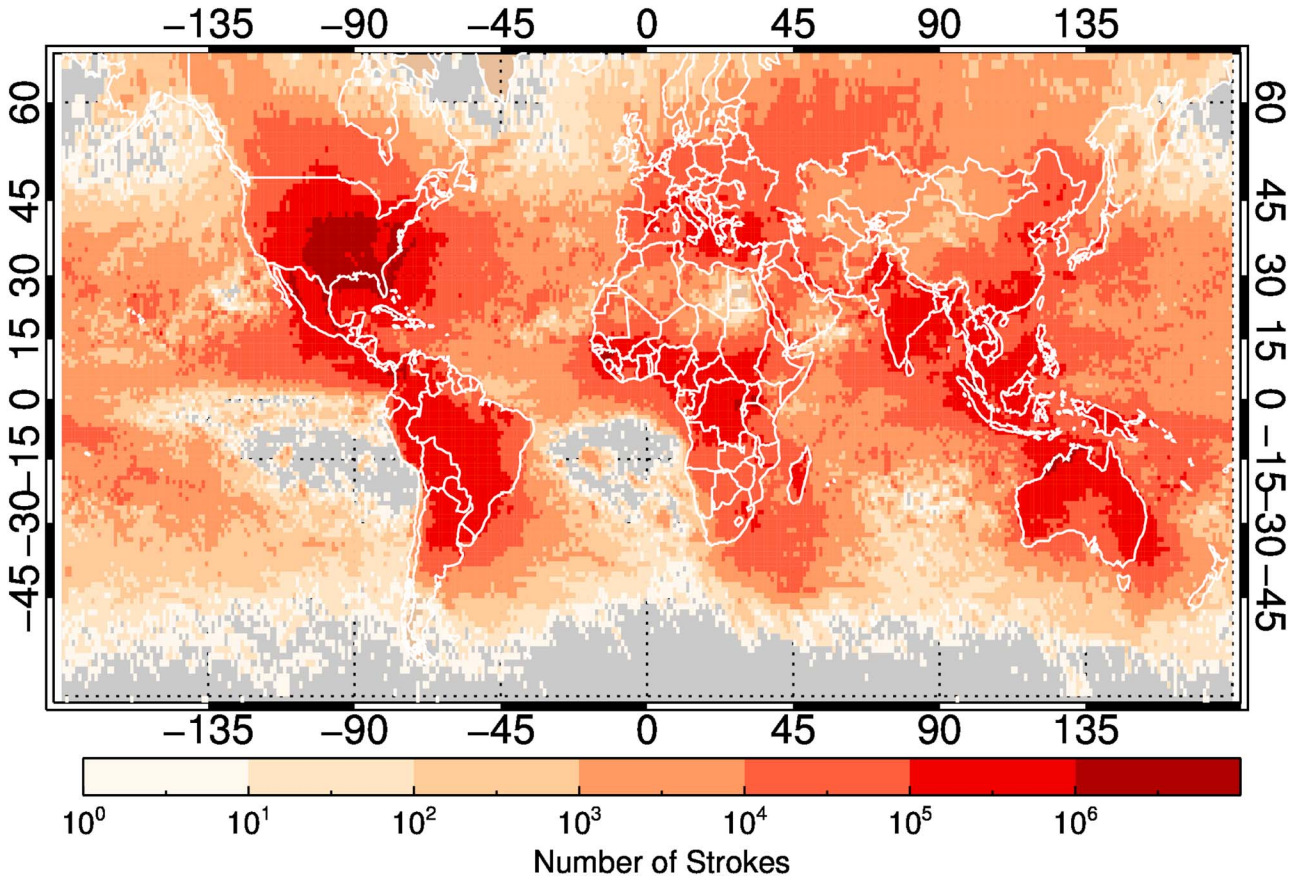

Figure 3. Distribution of the unique lightning discharges in 1° × 1° bins detected by ENTLN, Vaisala, and WWLLN using the unioned (i.e., merged) data set.

and supporting information figures, an estimate of the relative contributions of each LLS was determined. For example, there was an order of magnitude increase in the number of discharges detected in large parts of Asia when incorporating the Vaisala data over using just either ENTLN or WWLLN. There was a similar order of magnitude increase in the number of discharges detected over the southeastern United States when incorporating ENTLN data into the Vaisala data.

4. Discussion and Conclusions

The Bayesian methodology described herein provides a method in which three LLSs can be directly compared without assuming that any particular LLS detects all lightning. While the raw counts of the ENTLN and Vaisala networks were similar and WWLLN detected an order of magnitude fewer strokes, no one LLS reported more than 60% of the total number of detected strokes/pulses. Hence, this methodology provides a more complete analysis of the performance of each network than can be obtained by pairwise, conditional probability comparisons.

We found that of the lightning strokes/pulses detected by ENTLN, Vaisala, and WWLLN, Vaisala detected 59.8%, ENTLN detected 56.8%, and WWLLN detected 7.9%. These are upper limits to the absolute detection efficiency of each LLS. Globally, the mean time and distance difference between the lightning discharges detected by these LLS were 1–4 μs and 4–6 km, suggesting that when lightning was detected, the time and location largely agree across the LLSs. The standard deviation in time differences was larger, 15–20 μs, while the standard deviation in the distance differences was similar to the mean difference.

The spatial variation of the performance of each LLS was different. While ENTLN detected more discharges in the northeastern United States and various spots around the world, Vaisala detected more lightning in northern South America and throughout Asia. In general, ENTLN performance was high in limited domains

throughout the world, consistent with locations that have a higher sensor density. Over the oceans, Vaisala generally detected more discharges than the other two LLSs, although there were locations such as off the eastern coast of South America in which WWLLN and/or ENTLN had a higher DE.

The temporal evolution of the individual absolute probabilities indicated that these can change on different scales. Because LLS performance, particularly for low-amplitude discharges, is highly determined by sensor density, a low-frequency trend in the absolute probability (and total counts) suggest a corresponding trend in the location of lightning activity relative to network sensors. One such example is the increase in the ENTLN probability from April to August, during North American summer. Since ENTLN has a high sensor density in this region [*Liu and Heckman*, 2012], the increase in ENTLN DE at this time is likely related to the increase in lightning activity during North American summer. The greater total number of discharges detected by ENTLN, relative particularly to Vaisala, supports this statement. Although there was an upgrade to NLDN in August 2015 [*Nag et al.*, 2016], resulting in a sustained increase in the number of discharges detected, the Vaisala DE at the beginning of November 2014 and the end of October 2015 is similar. This can be further explored as these data sets continue to grow. There was also high-frequency (day-to-day) variability in the probabilities; this may be due to variations in LLS performance (e.g., due to ill-performing sensors). Detailed investigations utilizing this methodology can evaluate this on localized regions.

By using the Bayesian analysis, the union of the multiple LLSs can be used to provide a more complete picture of lightning activity. We found that these three LLSs detected 2.842×10^9 unique strokes/pulses for this 1 year time period, an average of 90.1 strokes/s. The conditional probabilities relating ENTLN and Vaisala indicate that there were unique discharges in each data set; this is especially the case spatially, as Figure 1 illustrates. In addition, WWLLN contributed a number of unique discharges off the east coast of South America and other oceanic areas. When using ground-based LLSs, assimilating the data sets can help offset the varying detection efficiencies (due to, for example, varying sensor densities) and produce a better view of all the lightning that occurs.

In addition, the spatial distribution of the counts (Figure 3) generally yielded the "three chimneys" [*Williams and Sátori*, 2004] often found in global lightning maps. This is broadly similar to the map of the global lightning activity from the Optical Transient Detector (OTD) and Lightning Imaging Sensor (LIS) data (Figure 2) [*Cecil et al.*, 2012]. Although this is not a direct comparison since the OTD/LIS data set [*Cecil et al.*, 2014] uses flashes while this analysis uses strokes/pulses, the two distributions agree on local maxima of lightning activity. One immediate difference is the location of the global maximum. This is located in North America for strokes; however, this likely reflects the higher detection efficiency of intracloud pulses due to higher sensor density. Since this work is based on 1 year of ground-based LLSs, future analyses using longer time periods will enable more robust comparisons.

In general, the union of the data sets provided by the Bayesian analysis can also be used to merge data from LLSs that vary in spatial performance or type of discharge (e.g., cloud to ground and intracloud). As suggested, this may provide better information when incorporating space-based observations of lightning, such as those that will be provided by the Geostationary Lightning Mapper and the Lightning Imager. Since these instruments will likely be more sensitive to intracloud lightning, merging data from a ground-based LLS (or multiple LLSs) more sensitive to cloud-to-ground lightning will yield a more detailed partitioning of total lightning.

Acknowledgments
This study was partially supported by NOAA grant Z7813005 (Cooperative Institute for Climate and Satellites-CICS) at the University of Maryland/ESSIC as part of the GOES-R Risk Reduction Research and NASA grant NNM05AA22A. We appreciate the comments and suggestions from two anonymous reviewers that greatly improved the manuscript. We thank Ryan Said of Vaisala for many helpful comments about the Vaisala data sets and providing postprocessed GLD360 data. ENTLN data were provided by Stan Heckman and Christopher Sloop. WWLLN data were provided by the University of Washington through an agreement with the GLM Science Team. NLDN data were provided to the NASA Lightning Imaging Sensor (LIS) instrument team and the NASA LIS Data Center via the NASA EOSDIS Global Hydrology Resource Center (GHRC) DAAC located at the Global Hydrology and Climate Center (GHCC), Huntsville, Alabama, through a license agreement with the Vaisala Group. The data available from the NASA EOSDIS GHRC DAAC are restricted to collaborators that have a working relationship with the NASA Marshall Space Flight Center (MSFC) Lightning Group.

References

Abarca, S. F., K. L. Corbosiero, and T. J. Galarneau Jr. (2010), An evaluation of the Worldwide Lightning Location Network (WWLLN) using the National Lightning Detection Network (NLDN) as ground truth, *J. Geophys. Res.*, *115*, D18206, doi:10.1029/2009JD013411.

Bitzer, P. M., J. C. Burchfield, and H. J. Christian (2016), A Bayesian approach to assess the performance of lightning detection systems, *J. Atmos. Oceanic Technol.*, *33*(3), 563–578, doi:10.1175/JTECH-D-15-0032.1.

Blakeslee, R. J., D. M. Mach, M. G. Bateman, and J. C. Bailey (2014), Seasonal variations in the lightning diurnal cycle and implications for the global electric circuit, *Atmos. Res.*, *135*, 228–243, doi:10.1016/j.atmosres.2012.09.023.

Boccippio, D., K. Cummins, H. Christian, and S. Goodman (2001), Combined satellite-and surface-based estimation of the intracloud-cloud-to-ground lightning ratio over the continental United States, *Mon. Weather Rev.*, *129*(1), 108–122.

Briggs, M. S., et al. (2013), Terrestrial gamma-ray flashes in the Fermi era: Improved observations and analysis methods, *J. Geophys. Res. Space Physics*, *118*, 3805–3830, doi:10.1002/jgra.50205.

Bruning, E. C., and D. R. MacGorman (2013), Theory and observations of controls on lightning flash size spectra, *J. Atmos. Sci.*, *70*(12), 4012–4029, doi:10.1175/JAS-D-12-0289.1.

Calhoun, K. M., D. R. MacGorman, C. L. Ziegler, and M. I. Biggerstaff (2013), Evolution of lightning activity and storm charge relative to dual-Doppler analysis of a high-precipitation supercell storm, *Mon. Weather Rev.*, *141*(7), 2199–2223, doi:10.1175/MWR-D-12-00258.1.

Calhoun, K. M., T. M. Smith, D. M. Kingfield, J. Gao, and D. J. Stensrud (2014), Forecaster use and evaluation of real-time 3DVAR analyses during severe thunderstorm and tornado warning operations in the hazardous weather testbed, *Weather Forecasting*, *29*(3), 601–613, doi:10.1175/WAF-D-13-00107.1.

Carey, L. D., and S. A. Rutledge (2003), Characteristics of cloud-to-ground lightning in severe and nonsevere storms over the central United States from 1989–1998, *J. Geophys. Res.*, *108*(D15), 4483, doi:10.1029/2002JD002951.

Cecil, D. J., D. E. Buechler, and R. J. Blakeslee (2012), Gridded lightning climatology from TRMM-LIS and OTD: Dataset description, *Atmos. Res.*, *135*, 404–414, doi:10.1016/j.atmosres.2012.06.028.

Cecil, D. J., D. E. Buechler, and R. J. Blakeslee (2014), *LIS/OTD Gridded Lightning Climatology Data Collection*, doi:10.5067/LIS/LIS-OTD/DATA311, data set available online from the NASA Global Hydrology Resource Center DAAC.

Christian, H., et al. (2003), Global frequency and distribution of lightning as observed from space by the Optical Transient Detector, *J. Geophys. Res.*, *108*(D1), 4005, doi:10.1029/2002JD002347.

Connaughton, V., et al. (2010), Associations between Fermi gamma-ray burst monitor terrestrial gamma ray flashes and sferics from the World Wide Lightning Location network, *J. Geophys. Res.*, *115*, A12307, doi:10.1029/2010JA015681.

Cummer, S. A., W. A. Lyons, and M. A. Stanley (2013), Three years of lightning impulse charge moment change measurements in the United States, *J. Geophys. Res. Atmos.*, *118*, 5176–5189, doi:10.1002/jgrd.50442.

Cummins, K., and M. Murphy (2009), An overview of lightning locating systems: History, techniques, and data uses, with an in-depth look at the US NLDN, *IEEE Trans. Electromagn. Compat.*, *51*(3), 499–518.

DeMaria, M., R. T. DeMaria, J. A. Knaff, and D. Molenar (2012), Tropical cyclone lightning and rapid intensity change, *Mon. Weather Rev.*, *140*(6), 1828–1842, doi:10.1175/MWR-D-11-00236.1.

Goodman, S. J., et al. (2013), The GOES-R Geostationary Lightning Mapper (GLM), *Atmos. Res.*, *125–126*, 34–49, doi:10.1016/j.atmosres.2013.01.006.

Jerauld, J., V. A. Rakov, M. A. Uman, K. J. Rambo, D. M. Jordan, K. L. Cummins, and J. A. Cramer (2005), An evaluation of the performance characteristics of the U.S. National Lightning Detection Network in Florida using rocket-triggered lightning, *J. Geophys. Res.*, *110*, D19106, doi:10.1029/2005JD005924.

Kitagawa, N., and M. Brook (1960), A comparison of intracloud and cloud-to-ground lightning discharges, *J. Geophys. Res.*, *65*(4), 1189–1201.

Koshak, W. J., K. L. Cummins, D. E. Buechler, B. Vant-Hull, R. J. Blakeslee, E. R. Williams, and H. S. Peterson (2015), Variability of conus lightning in 2003–12 and associated impacts, *J. Appl. Meteorol. Climatol.*, *54*(1), 15–41, doi:10.1175/JAMC-D-14-0072.1.

Liu, C., and S. Heckman (2012), Total lightning data and real-time severe storm prediction. paper presented at 10th Session Conference on Meteorological Environmental Instruments and Methods of Observation Management Group, World Meteorological Organization, Brussels, Belgium.

Lu, G., S. A. Cummer, R. J. Blakeslee, S. Weiss, and W. H. Beasley (2012), Lightning morphology and impulse charge moment change of high peak current negative strokes, *J. Geophys. Res.*, *117*, D04212, doi:10.1029/2011JD016890.

MacGorman, D. R., D. W. Burgess, V. Mazur, W. D. Rust, W. L. Taylor, and B. C. Johnson (1989), Lightning rates relative to tornadic storm evolution on 22 May 1981, *J. Atmos. Sci.*, *46*(2), 221–251, doi:10.1175/1520-0469(1989)046<0221:LRRTTS>2.0.CO;2.

Mach, D. M., R. J. Blakeslee, and M. G. Bateman (2011), Global electric circuit implications of combined aircraft storm electric current measurements and satellite-based diurnal lightning statistics, *J. Geophys. Res.*, *116*, D05201, doi:10.1029/2010JD014462.

Mallick, S., et al. (2015), Performance characteristics of the ENTLN evaluated using rocket-triggered lightning data, *Electr. Power Syst. Res.*, *118*, 15–28, doi:10.1016/j.epsr.2014.06.007.

Nag, A., et al. (2011), Evaluation of U.S. National Lightning Detection Network performance characteristics using rocket-triggered lightning data acquired in 2004–2009, *J. Geophys. Res.*, *116*, D02123, doi:10.1029/2010JD014929.

Nag, A., M. J. Murphy, W. Schulz, and K. L. Cummins (2015), Lightning locating systems: Insights on characteristics and validation techniques, *Earth Space Sci.*, *2*(4), 65–93, doi:10.1002/2014EA000051.

Nag, A., M. J. Murphy, and J. A. Cramer (2016), Update to the U.S. National Lightning Detection Network. paper presented at 24th International Lightning Detection Conference Proceedings.

Poelman, D. R., W. Schulz, and C. Vergeiner (2012), Performance characteristics of distinct lightning detection networks covering Belgium, *J. Atmo. Oceanic Technol.*, *30*(5), 942–951, doi:10.1175/JTECH-D-12-00162.1.

Pohjola, H., and A. Mäkelä (2013), The comparison of GLD360 and EUCLID lightning location systems in Europe, *Atmos. Res.*, *123*, 117–128, doi:10.1016/j.atmosres.2012.10.019, 6th European Conference on Severe Storms 2011. Palma de Mallorca, Spain.

Reeve, N., and R. Toumi (1999), Lightning activity as an indicator of climate change, *Q. J. R. Meteorol. Soc.*, *125*(555), 893–903, doi:10.1002/qj.49712555507.

Rodger, C. J., J. B. Brundell, and R. L. Dowden (2005), Location accuracy of VLF World-Wide Lightning Location (WWLL) network: Post-algorithm upgrade, *Ann. Geophys.*, *23*(2), 277–290, doi:10.5194/angeo-23-277-2005.

Rubinstein, M. (1994), On the estimation of the stroke detection efficiency by comparison of adjacent lightning location systems, paper presented at 22nd International Conference on Lightning Protection, Budapest, Hungary.

Rudlosky, S. D. (2015), Evaluating ENTLN performance relative to TRMM/LIS, *J. Oper. Meteorol.*, *3*(2), 11–20.

Rudlosky, S. D., and D. T. Shea (2013), Evaluating WWLLN performance relative to TRMM/LIS, *Geophys. Res. Lett.*, *40*, 2344–2348, doi:10.1002/grl.50428.

Said, R. K., and M. Murphy (2016), GLD360 upgrade: Performance analysis and applications. paper presented at 24th International Lightning Detection Conference Proceedings.

Said, R. K., U. S. Inan, and K. L. Cummins (2010), Long-range lightning geolocation using a VLF radio atmospheric waveform bank, *J. Geophys. Res.*, *115*, D23108, doi:10.1029/2010JD013863.

Said, R. K., M. B. Cohen, and U. S. Inan (2013), Highly intense lightning over the oceans: Estimated peak currents from global GLD360 observations, *J. Geophys. Res. Atmos.*, *118*, 6905–6915, doi:10.1002/jgrd.50508.

Schultz, C., W. Petersen, and L. Carey (2009), Preliminary development and evaluation of lightning jump algorithms for the real-time detection of severe weather, *J. Appl. Meteorol. Climatol.*, *48*(12), 2543–2563.

Schultz, C. J., L. D. Carey, E. V. Schultz, and R. J. Blakeslee (2015), Insight into the kinematic and microphysical processes that control lightning jumps, *Weather Forecasting*, *30*(6), 1591–1621, doi:10.1175/WAF-D-14-00147.1.

Steiger, S. M., R. E. Orville, and L. D. Carey (2007), Total lightning signatures of thunderstorm intensity over North Texas. Part I: Supercells, *Mon. Weather Rev.*, *135*(10), 3281–3302, doi:10.1175/MWR3472.1.

Thomas, R., P. Krehbiel, W. Rison, T. Hamlin, D. Boccippio, S. Goodman, and H. Christian (2000), Comparison of ground-based 3-dimensional lightning mapping observations with satellite-based LIS observations in Oklahoma, *Geophys. Res. Lett.*, *27*(12), 1703–1706.

Thompson, K. B., M. G. Bateman, and L. D. Carey (2014), A comparison of two ground-based lightning detection networks against the satellite-based Lightning Imaging Sensor (LIS), *J. Atmos. Oceanic Technol.*, *31*(10), 2191–2205, doi:10.1175/JTECH-D-13-00186.1.

Virts, K. S., J. M. Wallace, M. L. Hutchins, and R. H. Holzworth (2015), Diurnal and seasonal lightning variability over the Gulf Stream and the Gulf of Mexico, *J. Atmos. Sci.*, *72*(7), 2657–2665, doi:10.1175/JAS-D-14-0233.1.

Williams, E. (2005), Lightning and climate: A review, *Atmos. Res.*, *76*, 272–287, doi:10.1016/j.atmosres.2004.11.014.

Williams, E., and G. Sátori (2004), Lightning, thermodynamic and hydrological comparison of the two tropical continental chimneys, *J. Atmos. Sol. Terr. Phys.*, *66*(13–14), 1213–1231, doi:10.1016/j.jastp.2004.05.015.